Received: 27 March 2018 | Revised: 30 May 2018 | Accepted: 22 June 2018

DOI: 10.1002/pip.3066

RESEARCH ARTICLE

WILEY PROGRESS IN PHOTOVOLTAICS

One-type-fits-all-systems: Strategies for preventing potential-induced degradation in crystalline silicon solar photovoltaic modules

Alessandro Virtuani | Eleonora Annigoni | Christophe Ballif

École Polytechnique Fédérale de Lausanne (EPFL), Institute of Microengineering (IMT), Photovoltaics and Thin Film Electronics Laboratory, Neuchâtel CH-2000, Switzerland

Correspondence
Alessandro Virtuani, École Polytechnique Fédérale de Lausanne (EPFL), Institute of Microengineering (IMT), Photovoltaics and Thin Film Electronics Laboratory, Neuchâtel CH-2000, Switzerland.
Email: alessandro.virtuani@epfl.ch

Funding information
EOS Holding; Swiss Innovation Agency (Innosuisse—SCCER program)

Abstract

In this work, we investigate the relationship between potential-induced degradation (PID) and the bill of material used in module manufacturing. We manufacture samples with different combination of materials, using two types of solar cells (conventional vs PID-free c-Si cells), two types of ethylene-vinyl acetate (EVA) films with low/high resistivity, and two types of backsheets with, respectively, low/high breathability properties, and subject the mini-modules to extended PID testing. Our results clearly indicate that, when using a breathable polymeric backsheet, to have a "*PID-free*" module the combination of PID-free cells and high-resistive EVA encapsulants is recommendable. The use of a conventional c-Si cell in combination with a high-resistive EVA encapsulant is still more effective than the use of PID-free cells in combination with low-quality EVA. Further, our results initially show that the breathability properties of the backsheet have apparently no influence on PID degradation. A second set of experiments using sandwich structures with increased resistance properties to water ingress (ie, glass and backsheets with barrier layers as rear covers and an edge sealant), however, indicates that preventing or reducing the diffusion of moisture in the encapsulant layer plays a role in further mitigating the impact of PID. This finding is supported by simulations of moisture ingress in the sandwich structures. Finally, we show that the use of a glass rear cover—compared with a polymeric backsheet—does not contribute in worsening the PID effect. On the contrary, by reducing moisture ingress in the front encapsulant layer, it delays the occurrence of PID.

KEYWORDS

bill of material (BOM), crystalline silicon, performance, potential-induced degradation (PID), reliability

1 | INTRODUCTION

Potential-induced degradation (PID) of crystalline silicon (c-Si) PV modules is a *sneaky* degradation mechanism, which may seriously affect the performance and return on investment of PV installations.[1,2] Although reliable statistics about the incidence of the PID phenomenon do not exist, anecdotal evidences suggest that its incidence is relatively frequent in solar systems/modules realized in previous and recent years.

The reasons leading to PID degradation, as well as potential mitigating strategies, are multiple and interdependent.[3] These are related to the following:

(1) The specific *climatic conditions* of the installation site[4];

Alessandro Virtuani, Eleonora Annigoni and Christophe Ballif contributed equally to this work.

(2) The *electrical layout* (ie, mostly the grounding and polarity) of the PV array/string;

(3) The *inverter choice*;

(4) Module design aspects specific to the *mounting solution* (ie, the presence/absence of a frame or of back rails);

(5) Module design aspects specific to the *materials* (encapsulants, solar cells, glass, backsheet [BS], etc.) used in the fabrication of the sandwich.

In this contribution, we focus on the latter point and investigate the relationship between PID and the *bill of material* (BOM) used in module manufacturing, focusing on the mainstream technology of p-type crystalline silicon (c-Si), and highlighting the great commercial advantage for module manufacturers to offer solutions independent on inverter choice and electrical layout and, therefore, suitable for all systems. What we call a *one-type- fits-all-systems* module.

When coming to module assembly, several strategies related to the choice of the materials are offered to manufacturers, and their customers, to suppress or minimize the negative impact of PID on framed modules. In particular, the use of the following:

i. Specific "*PID-free*" cells. One strategy to suppress PID impact is to deposit dielectric anti-reflective coatings (ARC) with increased conductivity (and refractive index) on the solar cells in a way that the migration of ions (such as Na+) from the module glass into the *pn* junction when applying high voltages is avoided or drastically reduced.[5] However, a trade-off exists between cell efficiency and PID sensitivity when modifying the composition of this layer. Other strategies at the cell level focus on increased doping profiles, surface treatments (such as growing an intermediate SiO_2 layer between the Si and the AR coating), or ion implantation in the cell's emitter.[6,7]

ii. Encapsulating polymers with higher electrical resistivity (ρ) to prevent the diffusion of alkali metal ions from the glass cover into the cell. Several materials such as thermoplastic polyolefin, ionomer, or high-quality ethylene-vinyl acetate (EVA) have been shown to prevent or strongly moderate the insurgence of PID.[4,8-10]

iii. Special cover glasses with reduced Na content or different processing, such as chemically strengthened glasses.[4,11]

However, the efficacy and the cost-effectiveness of the single strategies (or their cross combination) are frequently unknown. In the present contribution, we investigate how PID degradation of encapsulated (and framed) solar cells is affected by the choice of the solar cell, and of the encapsulating polymer.

In view of the industrial application of the results and considering the constant market pressure to significantly abate module-manufacturing costs, we focus here on what are, as of today, the most cost-effective solutions only, and do not investigate for example the use of special cover glasses. For the same reason, as EVA is currently used in >90% of the modules manufactured today, we focus on this encapsulant only.

As the properties of the BS may have a strong impact on the physical properties of the encapsulant material (water content and resistivity), in our study we consider as well BSs with different breathability properties, ie, with different water vapor transmission rates (WVTR). To interpret some of the experimental results, we then run a second set of experiments, and in parallel perform some simulations, focused at investigating the influence on PID degradation of moisture ingress in the module sandwich.

2 | EXPERIMENTAL WORK AND MODELLING

2.1 | Influence of solar cell, encapsulant, and backsheet properties on PID

The materials that we use for assembling our test devices are all commercially available. These include two types of c-Si solar cells (conventional vs PID-free c-Si solar cells, both p-type), two types of EVA films from the same supplier with, respectively, low and high electrical resistivity, and two types of BS from the same supplier with, respectively, low and high breathability, ie, BS with different WVTRs. We then investigate all possible combinations (ie, $2^3 = 8$) of this BOM list and assemble, by means of a conventional lamination process, our one-cell mini-modules according to the matrix shown in Table 1. In order to simulate the presence of a frame, the edges of the mini-modules are covered with a conductive Al tape, as shown in Figure 1.

Additionally, we measure the volume resistivity of our encapsulants as a function of humidity and temperature. Before each measurement, the cured samples were pre-conditioned in a climatic chamber. Measurements are performed according to the IEC 62788-1-2 standard (Method B)[12] using a Keithley electrometer and an 8009 resistivity test fixture.

In a second set of experiments, we investigate further the role of the BS and of structures with increased resistance properties to water ingress. To do this, we manufacture mini-modules using conventional (std-cell) cells only and EVA with high volume resistivity (EVA-high-ρ) and make use of structures with increased resistance properties to water ingress: (1) glass/glass (G/G) and (2) glass/glass with edge sealant (G/G-seal). The rear glass and a desiccant-filled polyisobutylene-based edge sealant are used to prevent moisture ingress in the module sandwich. In order to verify that the rear cover glass is not contributing in worsening the PID effect, we manufacture an additional sample (3) using a fully impermeable BS that includes a laminated Al foil

TABLE 1 Overview of the different materials (cells, encapsulants, backsheets) used in the first part of the study

Bill of Material	* From Datasheet	
Cells	Standard c-Si (std-cell)	PID-free cell (PID-free)
Encapsulants	EVA high resistivity (EVA-high-ρ) *ρ> $1{\cdot}10^{15}$ Ω·cm	EVA low resistivity (EVA-low-ρ) *ρ> $6{\cdot}10^{14}$ Ω·cm
Backsheets	BS high WVTR (BS-high-B) *WVTR ~ 1.8 g/m^2/d	BS low WVTR (BS-low-B) *WVTR ~ 0.7 g/m^2/d

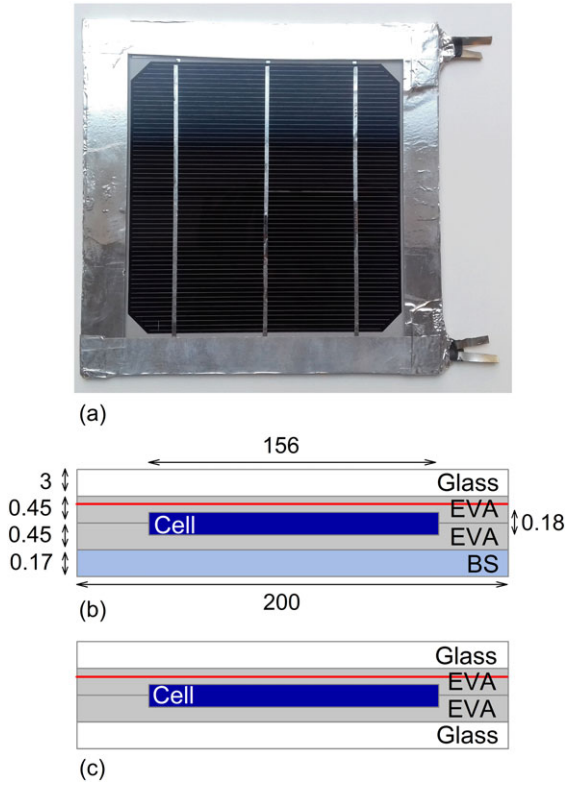

FIGURE 1 A, Top view of the 1-cell mini-modules used in this work with an Al tape applied to the edges simulating the presence of a frame. Cross sections of the two encapsulation configurations considered for simulating the water diffusion into the sandwich: B, 2D geometry employed in the FEM simulations for the glass/backsheet construction, and C, glass/glass structure. Thanks to vertical symmetry (impermeable front and rear cover), in the latter case, a simple 2D geometry of 200 × 200 mm^2 given by the only encapsulant is considered for the simulations [Colour figure can be viewed at wileyonlinelibrary.com]

barrier (G/BS-bar). All samples use a solar-grade front cover glass sheet. An overview of the rear covers used in this study is given in Table 2.

2.2 | PID stress tests

The samples are subjected to a PID stress test as prescribed by the relevant IEC Technical Specification for c-Si modules (IEC TS 62804-1:2015[13-15]) using a climatic chamber. Besides the conventional stress level (ie, 60°C, 85% RH, −1000 V, or 60/85), in a set of samples, we increase the stress level to 85°C, 85% RH (85/85) to accelerate the degradation. The test is run beyond the conventional 96 hours up to 192 hours, and for a much longer time in the second round of experiments. Before and after the degradation, the modules are characterized by means of IV measurements at standard test conditions (STC: 1000 W/m^2, 25°C, AM1.5).

2.3 | Modelling of water ingress in the sandwich structure

To interpret some experimental findings and investigate further the role of the BS and of water ingress on the evolution of PID, we then run some simulations of moisture diffusion in the sandwich structure using two different configurations shown in Figure 1B,C: a glass/BS structure and a glass/glass one.

We measure the WVTR used in the simulations of our materials at different temperatures, using a *Mocon Permatran twin 3/33* for the EVA and a *7001 Water Vapor Permeation Analyser* for the BS. For each material, we extract the water diffusion coefficient, the water solubility (used to estimate the water saturation concentration in the material), and their activation energies.

In a G/G module, water is able to penetrate from the edges into the unprotected encapsulant. We solve the diffusion equation in a 2D domain of length L_x and width L_y equal to 0.2 m (ie, the size of a one-cell mini-module) using the Fourier series shown in Equation 1, an approach previously used by Kempe et al and Jankovec et al.[16,17] In the equation, c_{init} and c_{surf} are, respectively, the initial and the surface concentration of the encapsulant (g/m^3), and D its diffusion coefficient (m^2/s).

$$c(x,y,t) = c_{surf} + (c_{init} - c_{surf}) \cdot \frac{16}{\pi^2} \cdot \sum_{n=0}^{\infty} \frac{1}{2n+1} \sin\left(\frac{(2n+1)\pi x}{L_x}\right) e^{-\frac{(2n+1)^2\pi^2}{L_x^2}Dt} \cdot \cdot \sum_{m=0}^{\infty} \frac{1}{2m+1} \sin\left(\frac{(2m+1)\pi y}{L_y}\right) e^{-\frac{(2m+1)^2\pi^2}{L_y^2}Dt} \quad (1)$$

The relative humidity (%) in the encapsulant is then obtained by using the calculated water concentration and setting RH = 100% when the saturation concentration c_{sat} is reached (Equation 2).[18]

$$RH(x,y,t) = \frac{c(x,y,t)}{c_{sat}} \cdot 100 \quad (2)$$

With respect to the G/BS configuration, the lack of vertical symmetry and the fact that we are interested in the RH in the front encapsulant, makes it necessary to employ finite elements method (FEM) simulations. An analytical 1D equation like the one proposed in Kempe et al[16] would, indeed, not be applicable here as it is rather suitable to estimate the RH in the rear encapsulant. The FEM

TABLE 2 Overview and WVTRs of the rear covers used in this study. All modules use a solar-grade front cover glass sheet

Rear Cover	WVTR, g/m^2/d * From datasheet	Edge Seal	Acronym
BS with high breathability	~ 1.8 * (at 23°C/85% RH)	-	BS-high-B
BS with low breathability	~ 0.7 * (at 23°C/85% RH)	-	BS-low-B
BS with Al foil barrier (no breathability)	< 5·10^{-3} * (at 38°C/90% RH)	-	BS-bar
Glass (no breathability)	0	-	G/G
Glass with edge seal (no breathability)	0	Y	G/G-seal

simulation are run with the software Comsol Multiphysics, with a 2D geometry as depicted in Figure 1B.

3 | RESULTS

3.1 | Resistivity measurements

Figure 1A shows the volume resistivity test preformed on the EVA-high-pand EVA-low-pencapsulants as a function of relative humidity. At room temperature (25°C) and RH 40%, the two encapsulants have a measured volume resistivity of $5{\cdot}10^{15}$ and $8.5{\cdot}10^{14}$, respectively, slightly higher than datasheet values. The volume resistivity is moderately reduced by increasing humidity.

The effect of temperature on ρ is much more pronounced than that of humidity, with ρ decreasing by approximately one order of magnitude over a 30°C interval (see Figure 2A). A similar behavior has been observed in other works (see, eg, Berghold et al19).

3.2 | PID testing at 60°C/85% RH

Table 3 shows the extent of power degradation (%) of our samples after PID testing at 60°C/85% RH. For *standard cells*, the choice of the EVA polymer has a drastic impact on PID degradation. Whereas the cells processed with a low resistivity polymer show a huge degradation (~ −80% after 96 and 192 hour), the ones processed with high-ρ EVA show nearly no degradation. This is true irrespective of the BS used in sample processing.

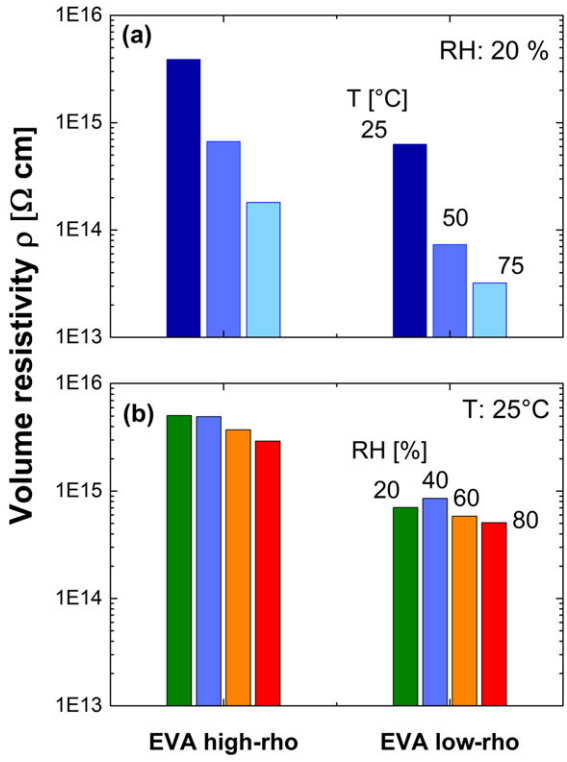

FIGURE 2 Volume resistivity for the EVA-high-pand EVA-low-pencapsulants as a function of (A) temperature at fixed RH (20%), and (B) of relative humidity at fixed temperature (25°C) [Colour figure can be viewed at wileyonlinelibrary.com]

Conversely, for the *PID-free cells*, the choice of the EVA, as well as of the BS, at 60°C/85% RH seems negligible, and for all the possible combinations of materials, the degradation after 96 and 192 hours is limited to ≤1%.

3.3 | PID testing at 85°C/85% RH

The picture changes when applying more severe test conditions accelerating the degradation. In Figure 3A,B and Table 3, we show the results of extended 85/85 (85°C/85% RH) PID testing on the samples manufactured, respectively, with conventional and PID-free c-Si cells.

For *conventional c-Si cells*, the choice of the EVA polymer has a drastic impact on PID degradation. Whereas the cells processed with a low resistivity polymer show a huge degradation (~ −90% after 96 hours), the ones processed with high-ρ EVA show a moderate degradation of −6.9% and − 11.7%, respectively, after 96 and 192 hours (for the BS-high-B samples). Surprisingly, in the extended testing (85/85), too, the effect of using BS with different WVTRs is nearly negligible. This aspect will be further investigated in Section 3.1.

For the PID-free cells (see Figure 3B), the choice of the EVA polymer has still a significant impact on PID degradation. Whereas the cells encapsulated with a high resistivity polymer show nearly no degradation (~ −1.5% after 96 and 192 hours), the ones processed with low-ρ EVA show a degradation of −12.1% and − 18.1%, respectively, after 96 and 192 hours (for the BS-high-B samples). This degradation, however, is larger than the one experienced by the samples processed with conventional c-Si cells and the high-ρ EVA polymer. For this set of samples, too, the progression of PID degradation is not affected by the breathability properties of the BS (see as well Section 3.1).

As the choice of the BS has apparently a negligible effect on PID degradation, to summarize these results, we bring together in Figure 4 —for the BS-low-B samples only—the results obtained for the samples with conventional cells and high-ρ EVA and for the ones including a PID-free cell (with high-ρ and low-ρ EVA).

The results of extended testing at 85/85 test conditions indicate that the use of PID-free cells is by far the best option to prevent the insurgence of PID, but only if the sandwich is processed in combination with a high resistive EVA polymer.

The use of a conventional c-Si cell in combination with a high-resistive EVA encapsulant still needs to be favored to the use of PID-free cells in combination with a low-quality EVA encapsulant.

If we stick to the IEC -5% pass/fail criterion, at 85/85 test conditions, however, the only samples experiencing a degradation below the threshold (after 96 and 192 hours), which will consequently pass the test, are the mini-modules assembled with PID-free cells in combination with the high-ρ EVA.

Conversely, for the 60/85 test conditions, all combinations of samples would pass the test (after 96 and 192 hours) with the exception of the conventional c-Si cells laminated with low-ρ EVA.

Nevertheless, we want to stress that these results were obtained on 1-cell mini-modules, so that, by considering the evolution of the PID phenomenon from the module edges (as frequently reported

TABLE 3 Power degradation of the different combination of samples after 96 and 192 hours of PID testing at (1) 60/85 and (2) 85/85 stress conditions (−1 kV)

Test Conditions >>		60°C/85% RH		85°C/85% RH	
Cells	EVA	BS high B (96/192 h) [%]	BS low B (96/192 h) [%]	BS high B (96/192 h) [%]	BS low B (96/192 h) [%]
Std c-Si cells	High ρ Low ρ	−0.7/−0.1 −85/−83.5	−0.8/−0.4 −77.9/−76	−6.9/−11.7 −89.1/−88.2	−9.2/−10.9 −96.6/−96
PID-free c-Si cells	High ρ Low ρ	−0.2/0 −0.7/−1	−0.3/−0.1 −1.7/−1	−1.6/−1.3 −12.1/−18.1	−1.8/−1.2 −11.7/−15.4

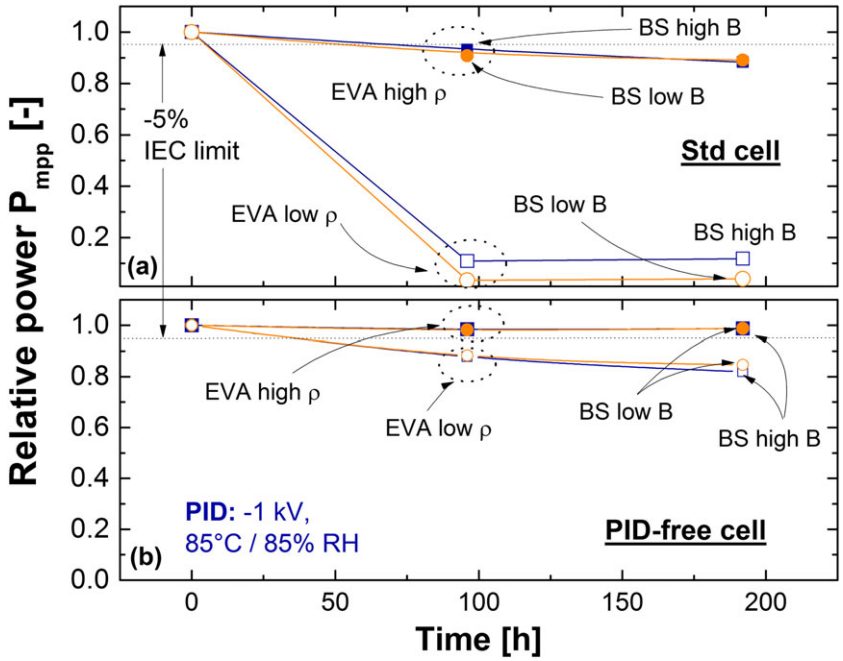

FIGURE 3 Degradation after PID test (85°C/85% RH, −1 kV) of encapsulated (A) standard (std) c-Si solar cells, and (B) "PID-free" solar cells. For both set of samples, two different EVA encapsulants with respectively a low and high resistivity ρ, and two types of backsheets, with a high and low breathability (B), have been used [Colour figure can be viewed at wileyonlinelibrary.com]

for fielded modules), they should represent a sort of worst-case situation, exhibiting an accelerated degradation. For this reason, sticking to the −5% IEC pass/fail threshold is possibly not meaningful with mini-modules.

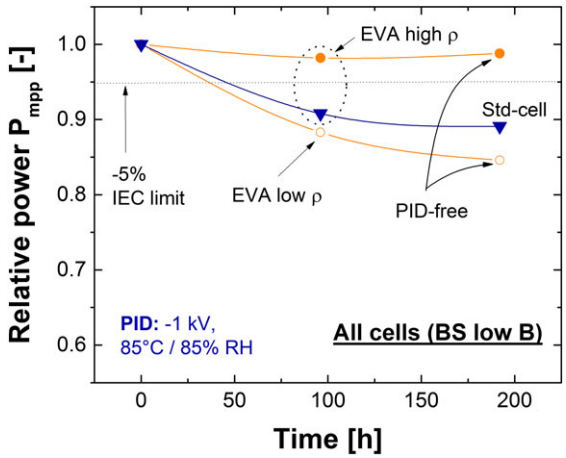

FIGURE 4 Degradation after PID test (85°C/85% RH, −1 kV) of standard (*std*) cells encapsulated with a high resistivity EVA, and of two "PID-free" cells processed with a low and a high ρ EVA encapsulant. All samples have a low breathability BS [Colour figure can be viewed at wileyonlinelibrary.com]

Consequently, the application of these results to 60- or 72-cell large-area modules is not straightforward; nevertheless, the results give a clear indication on the possibilities that are offered to mitigate the PID phenomenon at the module level.

Another result worth highlighting is that, apparently, the breathability properties of the BS have no significant influence on PID degradation at least under constant and relatively harsh stress conditions. As Figure 2B shows, the volume resistivity of EVA is reduced by increased the water content in the film, so that the latter finding is a bit counterintuitive (see Schulze et al,20 too), but is clarified with the water ingress simulations results presented in Section 3.1. Where we show that with the high levels of humidity used in the PID test (ie, 85% RH), the water diffusion dynamics experiences a moderate delay only of ~10 hours for the mini-modules encapsulated with, respectively, BSs with high and low WVTR.

Additionally, the generation of acetic acid during DH is a common degradation mechanism of EVA that may affect module's performance (yellowing/browning leading to reduced I_{sc}, and corrosion of ribbons/contacts leading to increased R_s and reduced FF). On the other hand, generally, the concentration of acetic acid starts to become significant after 2000 hours (or more) in DH (see Weber et al and Masuda et al21,22), depending on the formulation of the EVA, the BS used, and the position in the module. Our samples were tested only up to

~200 hours (and later to <600 hours, see Figure 5), and we never observed a reduction in current or an increase of R_S. So that we exclude the superposition of any additional degradation mechanism.

3.4 | Influence on PID degradation of moisture ingress in the module sandwich

To better understand the effect on the evolution of PID of the BS and of moisture ingress in the module sandwich, we run a second set of experiments manufacturing module structures with increased resistance properties to water ingress: (1) glass/glass (G/G) and (2) glass/glass with edge sealant (G/G-seal). The rear glass is used to prevent water ingress from the back, and the edge sealant to perfectly seal the module edges. In this respect, the latter sample can be considered as a reference sample fully impermeable to water ingress, at least for the first several hundreds of hours of exposure in a climatic chamber, before the edge seal is completely saturated with water.[23,24]

Additionally, to verify that the rear glass is not contributing in worsening the PID effect, we manufacture an additional sample (3) using an impermeable BS that includes a laminated Al foil barrier (G/BS-bar). The full set of mini-modules used in this second run of experiments is made using conventional cells only, and—in order to avoid the risk of an accelerated degradation, which would not allow distinguishing the contributions of the different rear covers—the EVA with high volume resistivity (EVA-high-ρ). All these samples are tested at 85/85 test condition with a duration extending up to 576 hours. The results are shown in Figure 5.

A clear difference is observed between sealed and non-sealed samples: with a power loss limited to −4.9%, the edge-sealed glass/glass experiences only a minor degradation after 576 hours of test. In the absence of an edge sealant, the power loss of the glass-glass sample is already −4.6% after 192 hours, and reaches −26% at 576 hours (ie, more than 5 times the degradation of the edge-sealed samples). We attribute this remarkable difference to moisture penetration from the edges—in the latter configuration—and diffusion over time into the front encapsulant of the unsealed G/G sample, with a consequent reduction of EVA's volume resistivity (see Figure 2B).

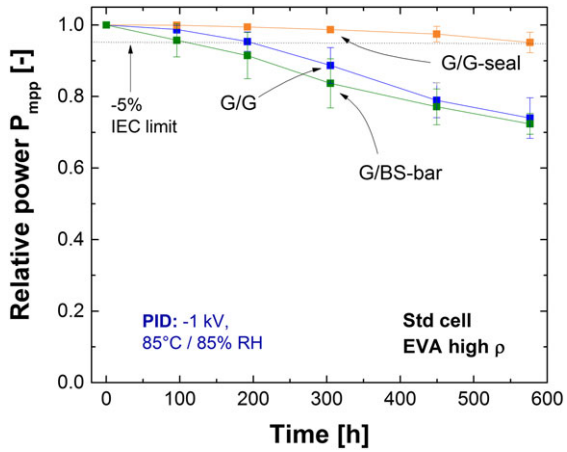

FIGURE 5 Degradation after exposure to PID test (85°C, 85% RH, −1 kV) of the mini-modules built with structures with different water-resistance properties: A glass/glass (G/G), glass/glass with edge sealant (G/G-seal), and a glass/backsheet that includes a laminated Al barrier foil (G/BS-bar). All samples are manufactured with conventional p-type c-Si solar cells and a highly resistive EVA [Colour figure can be viewed at wileyonlinelibrary.com]

In addition, we want to stress the fact that by preparing a mini-module with conventional c-Si cells and EVA with high volume resistivity in a glass/glass configuration, in combination with the use of an edge-sealant, we are able to realize a device that withstands the harsher 85/85 PID stress test conditions without nearly any observable degradation during the first 300 hours of test, and reaching the −5% IEC threshold after 576 hours. Because the time required to water to penetrate beyond a desiccant-filled polyisobutylene-based edge sealant at 85/85 conditions is typically around 5000 hours[23,24], we attribute this power degradation to the following: (1) progression of water ingress due to a possible loss of adhesion between the edge sealant and the glass, or (2) a late activation of the PID process in the presence of a very high resistivity encapsulant, or a combination of the two options.

Further, by directly comparing the impact of PID testing on the G/G and the G/BS-Al samples, we highlight as well the observation that the samples with a rear glass sheet do not suffer from increased degradation. Indeed, the degradation is comparable (or slightly lower) on the long run (>400 hours) and lower in the first 350 hours of test.

The p-type Si Al-BSF solar cells exposed to a negative voltage with respect to ground will still drive a migration of Na + ions from the rear glass pane to the cell. Nevertheless, these Na+ target the rear Al metallization of the cell, with no impact on PID, and not the ARC layer of the cell's front side nor the p-n junction. In this type of cells, it is in fact the drift of Na+ ions from the front glass and their accumulation on the ARC layer that can lead to the creation and decoration of stacking faults by the alkali metal ions. This will in turn induce a severe shunting of the p-n junction with a consequent degradation of overall cell performance.[25-28]

This model, for which consensus exists in describing PID degradation in mainstream Al-BSF p-type solar cells, does evidently not apply when the positively charged ions target the rear side metallization of the solar cells.

Finally, to summarize these last findings, we plot in Figure 6 the results for the first 192 hours of PID testing, highlighting the strong impact that the rear cover and the use of an edge sealant have on the evolution of the PID phenomenon.

On the long run (~580 hours of PID testing), nearly no difference could be observed in the degradation of the samples with an impermeable rear cover without the edge sealant (G/G and G/BS-bar, see Figure 5). For shorter stress times (192 hours), however, for these same samples, we observe a discrepancy that we cannot fully explain (see Figure 6).

3.5 | Modelling water ingress in the sandwich structure

In order to better understand the role of the BS and the results of Figures 3, 5, and 6, we run simulations of water ingress in the module sandwhich as described in Section 2.3. For both the G/G and G/BS configurations, the simulated water concentration is overestimated

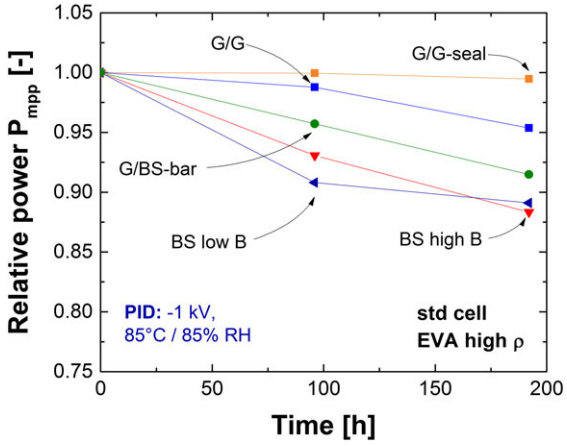

FIGURE 6 Evolution of PID degradation during the first 192 hours (85°C/85% RH, −1 kV) for all the mini-modules manufactured with conventional p-type c-Si solar cells and a highly resistive EVA. The different sandwich structures are: glass/glass (G/G), glass/glass with edge sealant (G/G-seal), and glass/backsheet including a laminated Al barrier foil (G/BS-bar), and the two samples with a conventional polymeric backsheet (with, respectively, a high and a low breathability B) [Colour figure can be viewed at wileyonlinelibrary.com]

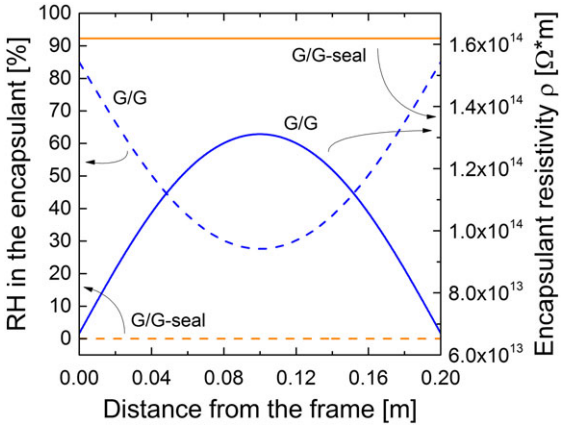

FIGURE 7 Water concentration (RH, dashed line) as a function of the distance from the edge in our 1-cell mini-modules after 576 hours of PID testing for the G/G and G/G-seal samples, and the corresponding EVA volume resistivity ρ (solid line) [Colour figure can be viewed at wileyonlinelibrary.com]

as the samples are framed by an aluminum tape, which is not taken into account in the boundary conditions.

For the G/G sample (cross-section displayed in Figure 1C), we simulate the water diffusion from the edges through the encapsulant during the PID test, in which the samples are exposed to environmental conditions of 85°C, 85% RH for 591 hours (ie, 576 + 15 hours of preconditioning).

To do this, we apply Equation (1) on a two-dimensional domain of width and length equal to 0.2 m (the size of a one-cell mini-module). The encapsulant is assumed to be initially dry (c_{init} = 0 g/m^3). As the high-resistivity EVA used in this work was not characterized in terms of diffusivity properties, we consider the diffusion coefficient D and the solubility S of an EVA polymer of which we measured the WVTR. We obtain a value of D = 8.13·10^{10} m^2/s at 85°C, in the range of what found by other authors for standard EVA encapsulants.[16,29] As boundary conditions, we set the four exposed surfaces in equilibrium with the chamber environmental conditions obtaining c_{surf} = c_{sat} = 4192 g/m^3 (ie, Henry law at 85°C, 85%).

These data are used to model the water concentration, and the relative humidity with (Equation (2)), in the EVA encapsulant layer of the G/G sample as a function of the distance from the edges, which is shown in Figure 7.

The correspondending resistivity ρof the encapsulant is then obtained as function of the internal RH according to the relation displayed in Figure 2 and is presented in Figure 7B, showing a considerable gradient from the edges (~6 × 10^{13} Ω·cm) to the center (~1.3 × 10^{14} Ω·cm) of the mini-modules.

For the G/G-seal sample (with edge sealant), we assume no water ingress throughout the whole duration of the test. The resistivity ρ of the encapsulant is therefore assumed to be constant over time all over the sample and equal to ~1.62 × 10^{14} Ω·cm (ie, ρ(85°C, 0%RH)).

For the case of a G/BS sample (BS-high-B), we simulate the water diffusion into the sandwich during the first 192 hours of PID testing by means of FEM, as described in Section 2.3. The BS and encapsulant are assumed initially dry, and their exposed surfaces in equilibrium with the chamber environmental conditions.

We then calculate the corresponding resistivity of the encapsulant along a line in the front EVA, at half distance between the EVA and the glass (see the red line in the cross-section presented in Figure 1B) and compare it to the one calculated for the corrsponding geometry of the glass/glass samples for which the rear glass acts as a perfect barrier to water ingress and moisture penetrates trough the encapsulant from the edges only. As shown in Figure 8, the mismatch in the distribution of ρ along the encapsulant layers for the two samples explains why the the evolution of PID dynamics in the G/G sample is slower than for the G/BS samples.

Similarly, for the same geometry of the G/BS sample, we run some simulations using two different BS properties corresponding to the BS with high and low breathability.

The results (not shown here) show that with the high levels of humidity employed in the PID test (ie, 85% RH), the water diffusion dynamics experiences a moderate delay only of ~10 hours for the

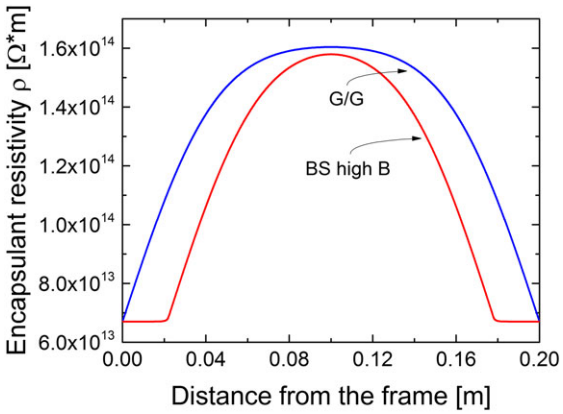

FIGURE 8 Encapsulant volume resistivity ρ as function of the distance from the frame after 192 hours of PID testing (85°C, 85% RH). The red and the blue curve refer, respectively, to the G/BS and the G/G configuration [Colour figure can be viewed at wileyonlinelibrary.com]

mini-modules encapsulated with, respectively, BSs with high and low WVTR.

This observation explains why for high levels of relative humidity (ie, during the execution of tests at 60/85 and 85/85 stress conditions for 96 hours and longer), no difference can be noticed for the samples having a BS with a high or low breathability.

4 | THE FUTURE OF PID

We observe that, even if the strategies to prevent/mitigate the insurgence of PID in modules using conventional Al-BSF p-type c-Si solar cells are now well understood, given the strong and constant market dynamics to bring down module manufacturing costs, we cannot guarantee that PID is not going to be observed in future field-deployed solar modules/systems. For this, we stress the importance that targeting consistent and reproducible module manufacturing practices, which start with a strict control of the BOM, have in preventing the later occurrence of failure mechanism in the field.

Similarly, we are confident that at modules level these approaches should equally be applicable to rapidly emerging technologies such as Passivated Emitter and Rear Cell, silicon-heterojunction or n-type solar cells, even when the degradation mechanism triggered by high potential differences in these devices may be completely different compared with conventional p-type solar cells.

In addition, given the industry downward pressure on costs, we highlight some cost considerations that might enable to select the best strategy to minimize PID. These include the following:

1. The potentially high cost for modified module glass, which makes this option difficult to be adopted;
2. As mentioned earlier, the considerable commercial advantage for module manufacturers to offer highly versatile solutions independent on inverter choice and electrical layout and, therefore, suitable for all system configurations: *one-type- fits-all-systems* modules;
3. At today's prices, the relatively low cost for using EVA encapsulants with higher volume resistivity (approximately, a +1% to 5% cost at module level), which, independently from the cell selection, has a considerable impact in preventing the insurgence of PID;
4. The observation that, even if alternative encapsulant materials known to prevent PID due to their high volume resistivity (such as PO, Ionomer, etc.) are considerably gaining momentum, EVA is still the encapsulant with the longest track-record and the widest market share in the industry ($\geq$ 90%), which makes it difficult to compete with in terms of prices.
5. At the cell level, the cost to manufacture *in-house* PID-free cells or to buy such cells might vary, even considerably, from one manufacturer to the other;
6. The additional potential advantage that the selection of materials/components less prone to favor water ingress in the sandwich structure (eg, glass/glass vs glass/BS, the use or not of edge seals) has on delaying PID dynamics.

5 | CONCLUSIONS

When using breathable BSs based on polymeric materials, our results clearly indicate that to have a "PID-free" module, the combination of PID-free cells and a high-resistive EVA encapsulants is the most recommendable choice. The use of a conventional c-Si cell in combination with a high-resistive EVA encapsulant is still more effective (and possibly constitutes a cheaper solution) than the use of PID-free cells in combination with low-quality EVA. For the less severe test conditions of 60°C/85% RH, the only combination of materials not passing the test (and showing a considerable degradation in performance, ie, ~80%) is that of conventional c-Si cells laminated with a low-ρ EVA.

The strong acceleration in PID degradation promoted by 85/85 rather than 60/85 stress conditions is explained by the considerable dependency of EVA's volume resistivity ρon temperature.

As resistivity measurements on EVA films indicate that ρ is reduced as well by increasing the water concentration in the film, we are initially surprised to observe that the breathability properties of the BS have apparently no influence on PID degradation—an observation that we are later able to explain by running some simulations of water diffusion in the encapsulant for different sandwich structures.

A second set of experiments using sandwich structures with increased resistance properties to water ingress (ie, glass and BS with barrier layers as rear covers and an edge sealant) indicates, in fact, that preventing or reducing the diffusion of moisture in the front encapsulant layer plays a role in further mitigating the impact of PID.

Finally, we highlight that

(1) by preparing a mini-module with conventional p-type c-Si cells and EVA with high volume resistivity in a glass/glass configuration, in combination with the use of an edge-sealant, we are able to realize a device that withstands the harsher 85/85 PID stress test conditions without nearly any observable degradation during the first 300 hours of test, and reaching the −5% IEC threshold after 576 hours;

(2) For the same type of cells, a glass rear cover—compared with a polymeric BS—does not contribute in worsening the PID effect. On the contrary, by reducing moisture ingress in the front encapsulant layer, it mitigates and delays the occurrence of PID.

ACKNOWLEDGEMENTS

This project is carried out within the frame of the Swiss Centre for Competence in Energy Research on the Future Swiss Electrical Infrastructure (SCCER-FURIES) with the financial support of the Swiss Innovation Agency (Innosuisse—SCCER program). Additionally, we gratefully acknowledge partial financial support from EOS Holding.

We are grateful to Xavier Niquille for support in sample manufacturing, to Jarle Austbo for the execution of measurements, and to all *PV-lab* team members. We are grateful to Jörg Horzel, Antonin Faes, and Matthieu Despeisse at CSEM for fruitful discussions and the delivery of testing material.

ORCID

Alessandro Virtuani http://orcid.org/0000-0001-5523-5200
Eleonora Annigoni http://orcid.org/0000-0003-0255-3031

REFERENCES

1. S. Pingel, O. Frank, M. Winkler, S. Daryan, T. Geipel, H. Hoehne, and J. Berghold, Potential induced degradation of solar cells and panels, in *Proc. of the 35th IEEE Photovoltaic Specialists Conference*, Honolulu, 2010, pp. 2817–2822.
2. P. Hacke, K. Terwilliger, R. Smith, S. Glick, J. Pankow, M. Kempe, S. Kurtz, I. Bennett, and M. Kloos, System voltage potential-induced degradation mechanisms in pv modules and methods for test, in Proc. of the 37th IEEE Photovoltaic Specialists Conference, Seattle, 2011, pp. 814–820;
3. Luo W, Khoo YS, Hacke P, et al. Potential-induced degradation in photovoltaic modules: a critical review. *Energ Environ Sci*. 2017;10(1):43-68.
4. Hoffmann S, Koehl M. Effect of humidity and temperature on the potential-induced degradation. *Prog Photovolt Res Appl*. 2014;22(2):173-179.
5. S. Koch, D. Nieschalk, J. Berghold, S. Wendlandt, S. Krauter, and P. Grunow, Potential induced degradation effects on crystalline silicon cells with various antireflective coatings, in *Proceedings of 27th EUPVSEC, Frankfurt*, 2012, pp. 1985–1990;
6. B. Braisaz, B. Commault, N. Le Quang, E. Gerritsen, M. Joanny, D. Binesti, G. Goaer, K. Radouane., Improved 1500 V PID resistance: encapsulants, cover glass and ion implanted cells, in Proc. of the *32nd European Photovoltaic Solar Energy Conference and Exhibition*, Munich, 2016, pp. 1874–1878;
7. W. Han, W. Shan, X. Niu, Q. Jiang, Y. Li, C. Lu, Z. Qiu, J. Li, Ion implantation—an effective solution to prevent c-Si PV module PID, in Proc. of the *28th European Photovoltaic Solar Energy Conference and Exhibition*, Paris, 2013, pp. 3309–3312;
8. J. Berghold, Koch, B. Frohmann, P. Hacke, and P. Grunow Properties of encapsulation materials and their relevance for recent field failures, in *Proc of the 40th IEEE Photovoltaic Specialists Conference*, 2014, pp. 1987–1992;
9. E. Annigoni, M. Jankovec, F. Galliano, H. Li, L. Perret-Aebi, M. Topic, F. Sculati-Meillaud, A. Virtuani and C. Ballif, Modeling potential-induced degradation (PID) in crystalline silicon solar cells: from accelerated-aging laboratory testing to outdoor prediction, in Proc. of the *32nd European Photovoltaic Solar Energy Conference and Exhibition*, Munich, 2016, pp. 1558–1563;
10. J. Kapur, A. Bennett, J. Norwood, B. Hamzavytehrany, and I. Kueppenbender, Tailoring ionomer encapsulants as a low cost solution to potential induced degradation, in *Proc. 28th European Photovoltaic Solar Energy Conference*, Paris, 2013, pp 476–479, 2013;
11. M. Kambe, K. Hara, K. Mitarai, S. Takeda, M. Fukawa, N. Ishimaru, M. Kondo, Chemically strengthened cover glass for preventing potential induced degradation of crystalline silicon solar cells, in Proc. of the 39th IEEE Photovoltaic Specialists Conference, Tampa, 2013, pp. 3500–3503;
12. IEC 62788–1-2:2016: "Measurement procedures for materials used in photovoltaic modules—Part 1-2: Encapsulants—Measurement of volume resistivity of photovoltaic encapsulants and other polymeric materials", IEC, Geneva;
13. IEC TS 62804–1:2015: "Photovoltaic (PV) modules—Test methods for the detection of potential-induced degradation—Part 1: Crystalline silicon", IEC, Geneva;
14. Hacke P, Smith R, Terwilliger K, Perrin G, Sekulic B, Kurtz S. Development of an IEC test for crystalline silicon modules to qualify their resistance to system voltage stress. *Prog Photovolt Res Appl*. 2014;22(7):775-783.
15. Hacke P, Spataru S, Terwilliger K, et al. Accelerated testing and modeling of potential-induced degradation as a function of temperature and relative humidity. *IEEE J Photovoltaics*. 2015;5(6):1549-1553.
16. Kempe MD. Modeling of rates of moisture ingress into photovoltaic modules. *Sol Ener Mater Sol Cells*. 2006;90(16):2720-2738.
17. Jankovec M, Galliano F, Annigoni E, et al. In-situ monitoring of moisture ingress in PV modules using digital humidity sensors. *IEEE J Photovoltaics*. 2016;6(5):1152-1159.
18. Coyle DJ. Life prediction for CIGS solar modules part 1: modeling moisture ingress and degradation. *Prog Photovolt Res Appl*. 2013;21(2):156-172.
19. J. Berghold, S. Koch, B. Frohmann, P. Hacke, and P. Grunow, Properties of encapsulation materials and their relevance for recent field failures, in Proc. of the 40th IEEE Photovoltaic Specialists Conference, Denver, 2014, pp. 1987 – 1992.
20. S. Schulze, A. Apel, R. Meitzner, M. Schak, C. Ehrich, J. Schneider, Influence of polymer properties on potential induced degradation of PV-modules, in Proc. of the *28th European Photovoltaic Solar Energy Conference and Exhibition*, Paris, 2013, pp. 503–507;
21. U. Weber, R. Eiden, C. Strubel, and N. Lenck, Acetic acid production, migration and corrosion effects in ethylene-vinyl-acetate- (EVA) based PV modules, in Proc. of the *29th European Photovoltaic Solar Energy Conference and Exhibition*, Amsterdam, 2014, pp. 3309–3312;
22. Masuda A, Uchiyama N, Hara Y. Degradation by acetic acid for crystalline Si photovoltaic modules. *Jap Jour App Phys*. 2015;54(4S):04DR04.
23. Kempe MD, Dameron AA, Reese MO. Evaluation of moisture ingress from the perimeter of photovoltaic modules. *Prog Photovolt Res Appl*. 2014;22(11):1159-1171.
24. Kempe MD, Panchagade D, Reese MO, Dameron AA, A A. Modeling moisture ingress through polyisobutylene-based edge-seals. *Prog Photovolt Res Appl*. 2015;23(5):570-581.
25. Harvey SP, Aguiar JA, Hacke P, Guthrey H, Johnston S, Al-Jassim M. Sodium accumulation at potential-induced degradation shunted areas in polycrystalline silicon modules. *IEEE J Photovoltaics*. 2016;6(6):1440-1445.
26. Naumann V, Hagendorf C, Grosser S, Werner M, Bagdahn J. Micro structural root cause analysis of potential induced degradation in c-si solar cells. *Energy Procedia*. 2012;27:1-6.
27. Naumann V, Lausch D, Hähnel A, et al. Explanation of potential-induced degradation of the shunting type by Na decoration of stacking faults in Si solar cells. *Sol Ener Mater Sol Cells*. 2014;120:383-389.
28. Naumann V, Lausch D, Graff A, et al. The role of stacking faults for the formation of shunts during potential induced degradation of crystalline Si solar cells. *Physica Status Solidi RRL*. 2013;7(5):315-318.
29. Hülsmann P, Heck M, Köhl M. Simulation of water vapor ingress into pv modules under different climatic conditions. *J Mater*. 2013;2013:1-7.

How to cite this article: Virtuani A, Annigoni E, Ballif C. One-type-fits-all-systems: Strategies for preventing potential-induced degradation in crystalline silicon solar photovoltaic modules. *Prog Photovolt Res Appl*. 2019;27:13–21. https://doi.org/10.1002/pip.3066